Graphene and 2D TMD material optical characterization with scanning probe microscopy

CHI Cheng (池骋)[1] & FANG ZheYu (方哲宇)[1,2*]

[1] *School of Physics, State Key Lab for Mesoscopic Physics, Academy for Advanced Interdisciplinary Studies, Peking University, Beijing 100871, China;*

[2] *Collaborative Innovation Center of Quantum Matter, Beijing 100871, China*

Received August 22, 2018; accepted October 26, 2018

Abstract Two-dimensional (2D) materials distinguish themselves by high specific surface areas and wide tunability in nanophotonics research. As the developing of 2D materials optical and opto-electronic investigations, scanning probe microscopy provides high spatial resolution and strong local field confinement, which can realize the single molecular and atomic level of characterization. Here, we review the nanophotonic and opto-electronic features of both pristine and hybrid 2D materials which are measured by scanning probe microscopy. The conclusion and prospective of scanning probe techniques for the future 2D materials characterization and practical applications are presented.

Keywords Two-dimensional materials; Scanning probe microscopy; Nanophotonics; Hybrid structures

doi: 10.16262/j.cnki.1005-0841.2018.04.001

1 Introduction

For two-dimensional (2D) materials, weak interlayer van der Waals bonding allows exfoliation to the monolayer, where the quantum confinement results in optical and electronic features different with that of bulk materials [1, 2]. These varied electronic properties can lead to a broad electromagnetic spectrum [3], and can be applied for non-deviation devices, etc. With a monolayer or few layers, most of 2D materials have strong optical response under incident illumination, and further boom the related opto-electronic applications.

Scanning probe microscopy (SPM) has been applied for 2D material characterization from different aspects. SPM has successfully resolved the molecular structure at the atomic level and measured the topography of 2D materials. The obtained spatial distribution of photon and electron state indicates material opto-electronic properties and contributes to understanding the underlying physical mechanism. On the other hand, the metallic scanning probe can couple to incident light, which leads to extreme localized field enhancement between the tip and material surface at the nanoscale. The responsive optical signal can reveal the molecular information and help in characterizing 2D material optical and structural properties.

In this review, we first introduce the principle and application of different SPM, and then the optical and opto-electronic properties of intrinsic graphene and hybrid TMD materials are summarized. Finally, a perspective of modern characterization methods for future 2D material investigation is given.

* Corresponding author (Email: zhyfang@pku.edu.cn)

2 The principle and application of SPM family

Scanning tunneling microscopy (STM) and atomic force microscopy (AFM) are two typical kinds of SPM, where the scanning tip with a different tip-sample feedback system can be controlled by either constant height mode or constant interaction mode [4]. The cantilever based tip is used for AFM, while the conducting probe is applied for STM. The nanoscale topography of 2D material flakes can be effectively obtained with AFM and STM measurements. On the other side, the optical and electronic properties of the 2D material can be investigated by using tip enhanced Raman scattering (TERS) and Kelvin probe force microscopy (KPFM), where the material surface potential and electron transfer process can be analyzed.

STM as a typical member of SPM family works with the feedback signal of tunneling current [5]. The wave functions of the scanning tip and sample atoms overlap in a close distance, which drive electrons tunneling through the energy barrier. This electron transfer generates the current between the tip and detected sample surface. In a standard operation, by keeping the current constant and measuring the displacement of the scanner, the surface topography can be obtained in atomic resolution. As shown in Fig. 1(a), the STM image of a thin graphene sheet (~1.5 nm thick) shows a clear honeycomb structure which has a good agreement with theoretical results [6]. Although STM technology is restricted to the conducting material, it has been effectively used to measure the topography of graphene and other 2D materials.

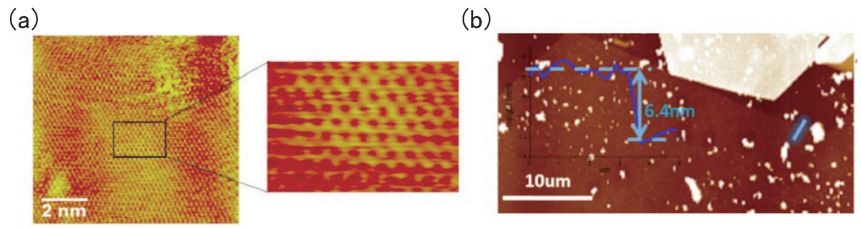

Figure 1 (a) STM image of a graphene flake. The atomic structure shows a hexagonal pattern [5]. (b) A typical AFM image of MoS_2 flake. The height profile indicates the sheet thickness of 6.4 nm.

In comparison with STM, AFM can be applied to measure all of the samples but with a lower spatial resolution. Instead of directly measuring the atomic force between the tip and sample, the AFM probe is attached to an elastic cantilever which can be used to reflect the diode laser. During the scanning of the sample, the force between the tip and surface can induce subtle bending in the cantilever. The corresponding shift of the reflected laser in the detection screen can describe the sample topography. AFM has been widely applied to measure the topography and height profile of 2D material flakes [7]. As shown in Fig. 1(b), the AFM image reflects the defect and thickness of MoS_2 monolayer as 6.4 nm.

TERS is a technique that combines STM and Raman spectroscopy, which is used to analyze the chemical structure of detected materials [8, 9]. Compared to the conventional surface enhanced Raman spectroscopy (SERS) [10—12], TERS can provide both strong localized field enhancement and high lateral resolution down to 10 nm, which depends on the tip size of the probe [13—16]. As shown in Fig. 2(a), the excitation laser couples to the TERS tip and forms a strong localized field in the detecting area. The scattering signal is collected by the objective lens in the far-field. The high spatial resolution property further develops the optical characterization of 2D materials at the nanoscale.

KPFM is an effective tool to measure the local contact potential difference between the AFM tip and the sample [18, 19]. The surface potential of the sample can be measured with a high spatial resolution, and its electronic properties of the sample surface can be characterized. A typical surface potential image of triangle MoS_2-WS_2 heterostructure is shown in Fig. 2(b). The work function difference of single-layer MoS_2 and bilayer WS_2 can be clearly observed [19], which can be used to explore the electron transfer process and related optoelectronic features of this heterostructure.

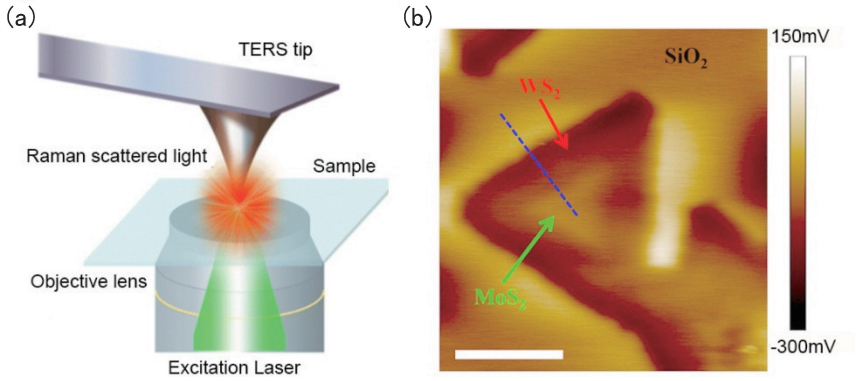

Figure 2 (a) Schematic of a typical TERS detection in the transmission mode. The localized field was effectively enhanced at LSP resonance. (b) KPFM image of MoS_2-WS_2 heterostructure on the SiO_2 substrate. Different material work functions lead to the observable surface potential distinction [17].

3 Pristine and hybrid 2D materials with SPM characterization

Graphene, as a special zero bandgap semi-metal 2D material, has a wide range of electronic and opto-electronic applications. On the other side, transition-metal dichalcogenides (TMD) monolayers are direct bandgap semiconductors with a strong light-matter interaction, which has potential applications for the opto-electronic devices. Both graphene and TMD materials are highly tolerant and chemically stable, thus are suitable candidates for the durable nanophotonic device in the future.

3.1 Pristine graphene

Graphene, as one of the most investigated 2D materials, has unique optical and electrical properties [20]. Scanning probe microscopy paves the way for the high spatial resolution study in graphene [21, 22], and provides an option in revealing its physical mechanism at the nanoscale.

Local strain of graphene relates tightly with the pseudo-magnetic field of the material and further modifies its electronic band structure, which impacts on both photoconductivity and photoresponse of graphene-based devices. Due to the diffraction-limit, the conventional Raman spectroscopy can be hardly used to study the local strain at the nanoscale. However, TERS with the tip size of tens of nanometers overcomes this limit and realizes a local measurement of strain in the graphene monolayer. As shown in Fig. 3(a), the position of strain can be clearly observed from the TERS mapping, and the type of strain is reflected by the G′ peak of Raman spectra. This study offers the method of characterizing the strain of graphene with a high spatial resolution, which contributes to the investigation of graphene quantum properties, and also the design of graphene-based opto-electronic devices.

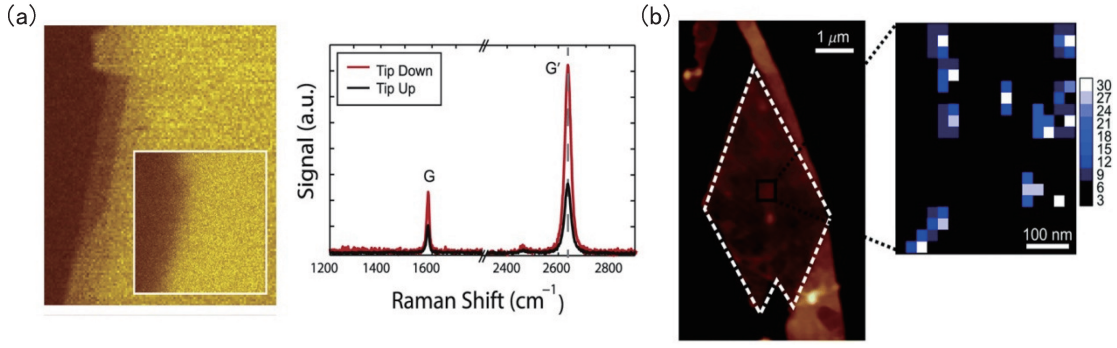

Figure 3 (a) Left: TERS mapping of graphene G′ band. Right: Raman scattering spectra of tip up/down two situations [23]. (b) Tip Enhanced Raman Mapping (TERM) of a monolayer graphene sheet. The Raman D-peak intensity image shows point defects [24].

Defects in graphene have aroused wide interest for their significant impact on the device performance [22, 23]. The conventional confocal microscopy has been widely utilized to study defects [25—27]. However it suffers the weakness in estimating the defect size, especially for the localized individual defect. SPM with the high spatial resolution provides an effective way to measure the point to point distance [28]. It was reported that the individual defect in graphene was successfully measured by TERS, as shown in Fig. 3(b). From the spectrum, we can see the value of I(D)/ I(G) has the positive correlation with the occurrence of defects. Both inter-defect distance and size of individual defects can be determined [29], which avoid potentially negative influence on the development of graphene-based devices. On the other side, these defects can also play the role of tuning graphene optical properties [30, 31]. In comparison with regular methods, i. e. the impurity introduction and bias doping, the defect tuning technique has the advantage in accuracy control at the nanoscale, which broadens the utilization of defects in graphene for the future opto-electronic device.

Besides the defect of graphene, other intrinsic discontinuities can also influence the material optical and electrical properties [32, 33]. Wrinkles, for example, can affect the graphene electron transport and limit the photoconductivity performance. In order to investigate the graphene wrinkles, TERS was introduced to characterize the optical and chemical properties of these discontinuities with a high resolution as shown in Fig. 4(a), where the G′ peak experienced a conspicuous intensity decreasing at the location of wrinkles [34]. This TERS study helps in understanding the structure curvature effect on graphene, further providing the method to avoid the potential influence of wrinkles on the future device application.

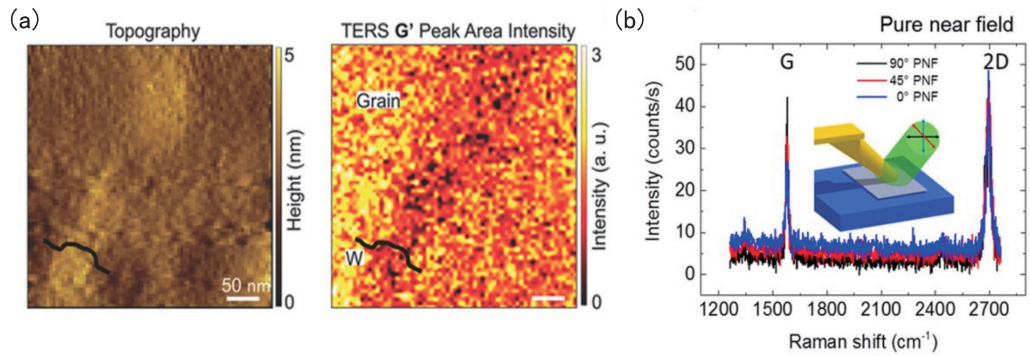

Figure 4 (a) Left: STM image of graphene wrinkle structure. Right: Corresponding TERS image of G′ peak intensity [34]. (b) TERS spectra of graphene in different tilted geometry in the near field [35].

In order to further investigate the selection rule, polarization-dependent TERS was performed on graphene, where corresponding peak intensities of G and G′ band changed enormously in the near field (Fig. 4(b)) [35, 36]. This result contradicts to the selection rule of the conventional Raman scattering [37], and suggests a quantum process of photon tunneling. It deepens the understanding of the TERS mechanism and broadens potential opto-electronic utilization of graphene as the substrate for the TERS measurement [38].

Graphene has also been used to investigate the plasmonic resonance in the THz region. The grain boundary and surface defect mentioned above play an important role in the scattering of surface plasmon polaritons (SPPs). To characterize the SPPs propagation in the graphene monolayer, the AFM tip was used to induce the SPPs excitation [39—42], and the tip-scattered near-field optical signal could be measured by the HgCdTe detector in the infrared region. As shown in Fig. 5(a), the graphene SPPs amplitude and phase information were collected by the modified AFM, from which we could tell the height of the graphene changed from monolayer to bilayer. In comparison with the monolayer, the SPPs propagation in the bilayer graphene has decreased amplitude and smaller excited wavelength [36, 37]. This study provides a comprehensive way of detecting and tuning the electronic structure of graphene at the nanoscale, and has potential in graphene-based plasmonic applications [43].

Similar to the intrinsic defect of graphene, edge effects can also impact on the plasmon behavior [46].

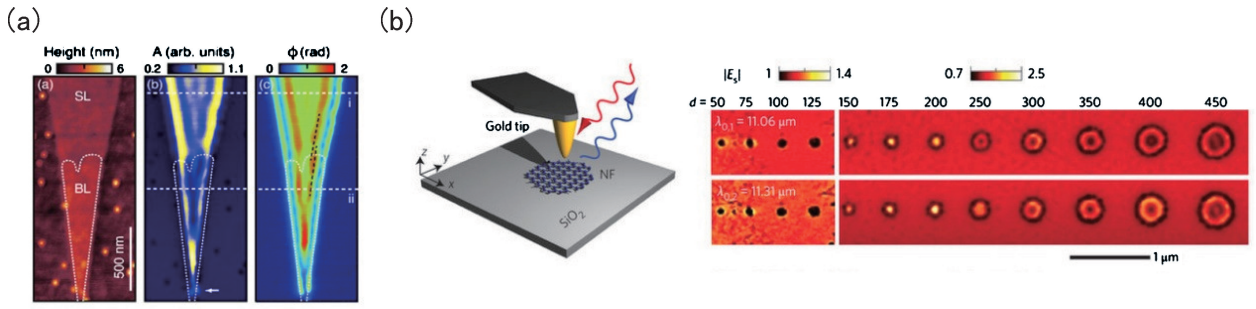

Figure 5 (a) Height, amplitude and phase maps of graphene nanoribbon [44]. (b) Schematic and results of real-space mapping graphene nanodisk plasmon modes experiment [45].

The generated plasmon resonance mode provides an effective confinement and enhancement of the localized field. In order to study these resonance modes, AFM-based near-field optical microscopy was applied, where the probe tip could be used to enhance the localized electromagnetic field. From Fig. 5(b), we can see that the plasmon near-field resonance changes with the diameter of the graphene nanodisk increasing from 50 to 450 nm, with its maximum intensity obtained at the diameter of 200 nm, and edge plasmon enhancement appears with the nanodisk diameter of 75 nm. This size difference indicates resonance modes distinction between the graphene sheet and edge, and opens up the investigation for edge modes of graphene by the real-space imaging technique.

3.2 Hybrid TMD materials

Compared to intrinsic graphene, hybrid 2D materials have a wider tunability in optical and electrical properties by introducing nanostructures with strong and functional tuning ability. By coupling with materials in different dimensions varying from 0D to 2D, hybrid structures show distinct and diversiform optical and opto-electronic properties for the device application.

Molecules as typical 0D materials, can bring various optical features and enrich hybrid structures properties [47—50]. For example, NiPc molecules were used to manipulate the PL response of WSe_2 monolayer by reducing their potential locations between the WSe_2 conduction and valence bands. From the AFM image of Fig. 6(a), the WSe_2 monolayer was functionalized by NiPc molecules [51]. Compared with the PL spectrum of pristine WSe_2, the WSe_2-NiPc hybrid presents a PL intensity decrease, which consists with the theoretical estimation. This PL tuning is reversible when NiPc molecules are rinsed from the WSe_2 monolayer, which indicates an active manipulation in TMD-based opto-electronic devices at the molecular level.

On the other side, semiconductor quantum dots (QDs) distinguish themselves by miscellaneousness and wide size-tunability [52, 53]. Hybrid structures of TMD materials and quantum dots can tailor the optical performance for the opto-electronic application [54]. As shown in Fig. 6(b), the WS_2 flake spin-coated by CdSe/ZnS QDs can be imaged by the AFM. In order to study the electron transfer in this hybrid structure, the transient absorption spectrum was measured. The result shows that electrons of QDs and holes from WS_2 can generate indirect excitons, which leads to an effective exciton coupling, and contributes to the design of hybrid 0D/2D heterostructures for the sensor device [55].

Compared to widely utilized semiconductor QDs, graphene QDs have a broad excitonic absorption band [59, 60], which satisfies the need for photovoltaic devices [61]. By applying the tip-induced method, the formative graphene QDs can confine electrons in the structure gap, and result in the enhancement of the local field. The spatial energy dependence can be probed by the tip-induced QD as shown in Fig. 6(c), which verifies electron behaviors of graphene QDs. This tip potential probing method helps in manipulating excitonic energy of graphene QDs, and broadens the applications of QDs in graphene-based opto-electronic devices [62, 63].

The electronic structure of graphene-metal hybrids was widely studied for opto-electronic applications [64, 65]. TERS was used to measure the optical response of graphene-Au nanoparticle (NP) hybrid

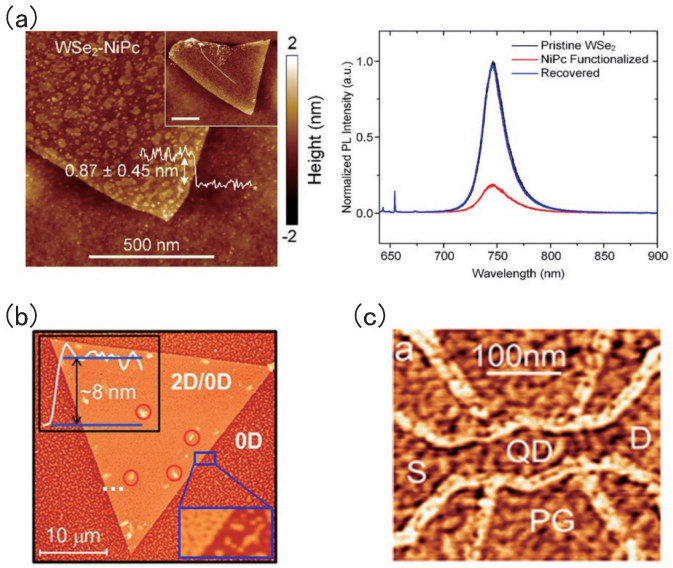

Figure 6 (a) Left: AFM image of Nickle Pc (NiPc) molecules adsorbed on the WSe_2 single layer; Right: PL intensity spectra of pristine WSe_2, WSe_2-NiPc and WSe_2 nanosheets after rinsing NiPc [56]. (b) AFM images of WS_2 nanosheet after being spin-coated by CdSe/ZnS nanodots. The height profile indicates the rising thickness of nanosheet from 0.7 to 8 nm after coating [57]. (c) Topography of a tip-induced graphene quantum dot [58].

structure, as shown in the left image of Fig. 7(a). From the TERS spectrum, we can see that electrons are effectively restrained by Au NPs on the graphene [66]. Compared with the graphene-metal hybrid, TMD-metal hybrids show a large tunability in opto-electronic properties. The TERS mapping of a MoS_2 envelope on Au nanotriangle structures shows that the brightest spots correspond to the strongest strain in the bending of MoS_2 monolayer (right image in Fig. 7(a)) [67], which indicates the application of strain-tuning in TMD-metal hybrids.

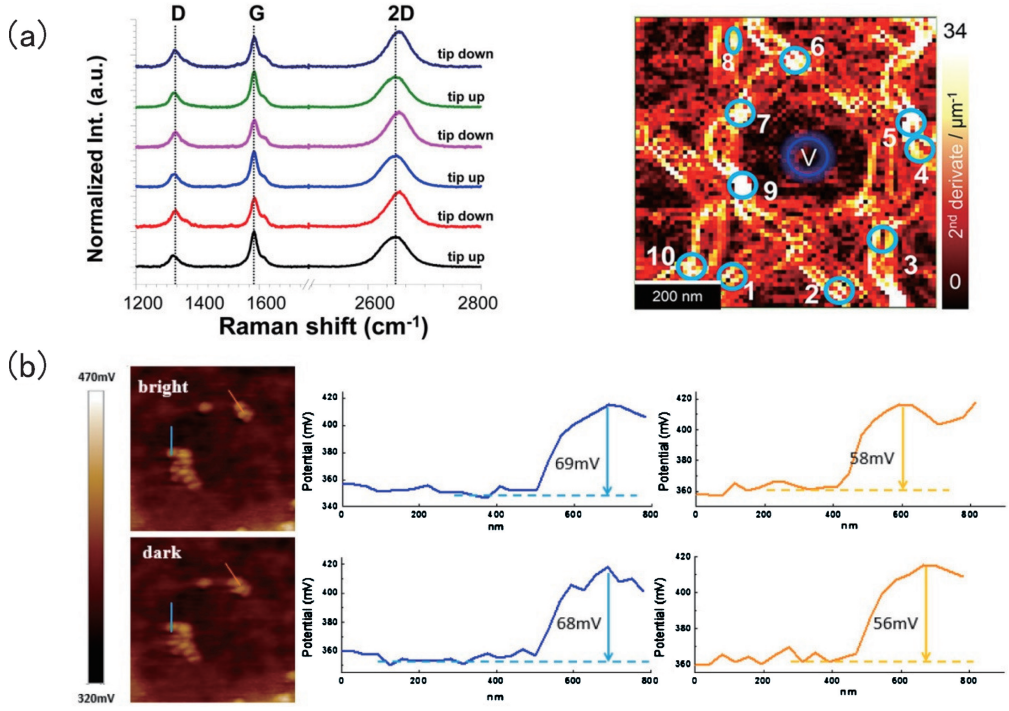

Figure 7 (a) Left: TERS spectra of graphene-Au NPs with and without tip away from Au NPs [66]. Right: TERS image of second order derivative points in MoS_2/Au nanotriangle hybrids [67]. (b) KPFM surface potential detection of Au-MoS_2 hybrid material. The thickness of MoS_2 is 18.4 nm [68].

By coupling with the metallic nanostructure, the PL of 2D materials can be manipulated. To investigate the effect of the electron injection process on the PL intensity, KPFM measurement was performed to obtain the surface potential of nanoflakes under different light illuminations (Fig. 7(b)) [68]. Together with PL results, it can be seen that the illumination affects less in the thinner MoS_2 flake than in the thicker one, which indicates that the electron transfer process from MoS_2 to Au NP dominates in the thinner flake, and results in the PL quenching. This study contributes to realizing PL tuning in metal-MoS_2 hybrids by manipulating the thickness of the nanosheet, thus helping in developing TMD-based opto-electronic devices [69].

Excitonic effects of TMD heterostructures have aroused attention for their wide optical applications [70, 71]. The topography of $MoSe_2$ on the bilayerd graphene (BLG) heterostructure surface is shown in Fig. 8(a), where the moire pattern of $MoSe_2$ monolayer misfits the lattice of $MoSe_2$/BLG. By measuring the PL of $MoSe_2$/BLG heterostructure at room temperature and 77 K [72], the 0.08 eV peak-shift was recorded, which indicated the rise of optical bandgap in the $MoSe_2$ monolayer induced by the BLG substrate. This experiment reveals the temperature-dependent peculiarity of exciton-hole excitation binding energy between the $MoSe_2$ and BLG.

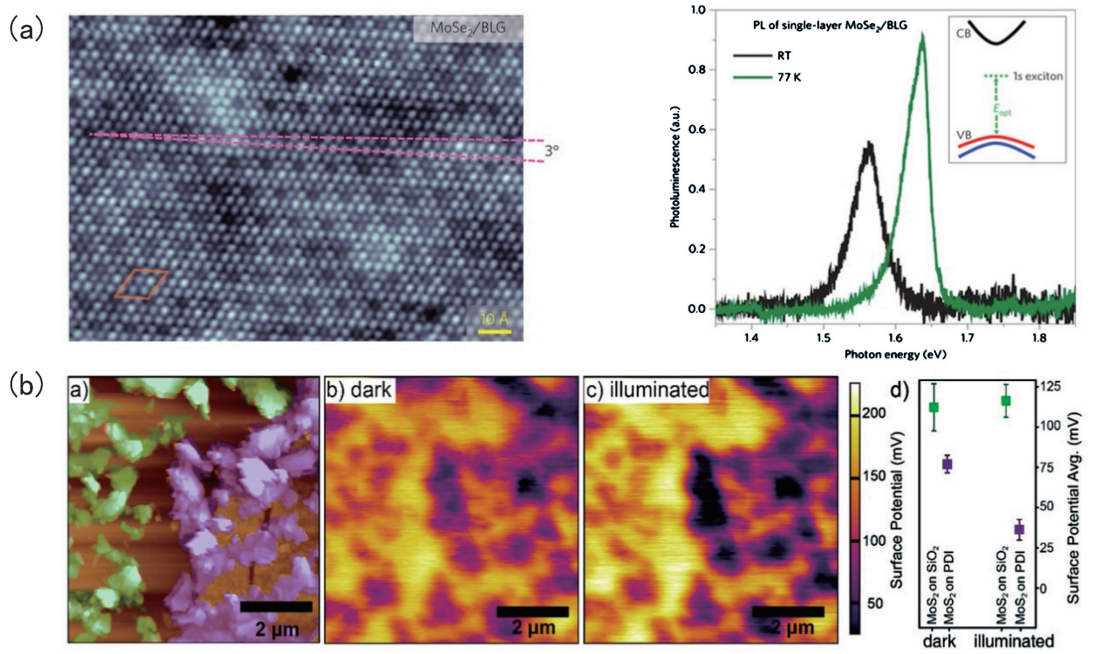

Figure 8 (a) Left: Topography of single-layer $MoSe_2$ on bilayer graphene. Distinction of $MoSe_2$ lattice and the Moire pattern has an angle of 3 degree. Right: PL measurements of $MoSe_2$/BLG monolayer at 77 K and room temperature, respectively [73]. (b) KPFM measurements of MoS_2 nanosheets on both glass and Dihexanoic acid-perylene-diimide (DHA-PDI) substrates, respectively [74].

TMD-organic heterojunctions, on the other side, are suitable candidates for photovoltaic applications because of their high tolerance and low preparation cost. The surface potential of MoS_2/DHA-PDI heterostructure was investigated by the KPFM [74]. As shown in Fig. 8(b), different heterostructures of MoS_2/PDI and MoS_2/SiO_2 were measured in the same square region with the size of 2 μm. The result shows that MoS_2/PDI has a decrease in the surface potential under illumination, while the MoS_2/SiO_2 heterostructure nearly remains the same, which suggests an efficient electron injection from MoS_2 to PDI under the incident illumination [75].

4 Conclusion and perspective

In the investigation of nanophotonic features of graphene and TMD materials, SPM plays an important role in providing high spatial resolution information of the nanostructure. For pristine graphene, its optical

and opto-electronic features are impacted by the edge effect and other intrinsic discontinuities, such as defects and wrinkles, which can be characterized and manipulated by SPM. For hybrid 2D materials, the stacked heterostructure can obtain a broad tuning ability compared with the intrinsic 2D monolayer. The hybrids in different dimensions were introduced and compared for the future opto-electronic device application, which were characterized by various SPM with high spatial resolution and enhanced electromagnet field at the nanoscale.

For the future research, advanced techniques are in need for a deeper looking of insight physics of 2D materials. Function integrations of SPM and other optical characterization methods are required for *in-situ* optical measurements in some extreme conditions. Besides TERS, the combination of PL and ultrafast lasers with STM can realize TEPL and THz-STM techniques, respectively [76, 77]. Other opto-electronic characterizations such as photocurrent and cathodoluminescence are candidates in scanning probe measurements of 2D materials [78]. These characterization methods have potential applications for the strong coupling of light-mater interaction, and can lead to an unprecedented future for the 2D material based opto-electronic devices.

Acknowledgements

This work was supported by the National Key Research and Development Program of China (Grant No. 2017YFA0205700), National Basic Research Program of China (Grant Nos. 2015CB932403 & 2017YFA0206000), National Natural Science Foundation of China (Grant Nos. 11674012, 61422501, 11374023 and 61521004), Foundation for the Author of National Excellent Doctoral Dissertation of China (Grant No. 201420), and National Program for Support of Top-notch Young Professionals (Grant No. W02070003).

References

[1] Geim A K, Grigorieva I V. Van der Waals heterostructures. Nature, 2013, 499: 419—425.
[2] Wang Q H, Kalantar-Zadeh K, Kis A, Coleman J N, Strano M S. Electronics and optoelectronics of two-dimensional transition metal dichalcogenides. Nat Nanotechnol, 2012, 7: 699—712.
[3] Xia F, Wang H, Xiao D, Dubey M, Ramasubramaniam A. Two-dimensional material nanophotonics. Nature Photonics, 2014, 8: 899—907.
[4] Kuhnke K, Grosse C, Merino P, Kern K. Atomic-scale imaging and spectroscopy of electroluminescence at molecular interfaces. Chem Rev, 2017, 117: 5174—5222
[5] Su C Y, Lu A Y, Xu Y P, Chen F R, Khlobystov N A, Li L J. High-quality thin graphene films from fast electrochemical exfoliation. ACS Nano, 2011, 5: 2332—2339.
[6] Wu X, Shao Y, Liu H, Feng Z, Wang Y L, Sun J T, Liu C, Wang J O, Liu Z L, Zhu S Y, Wang Y Q, Du S X, Shi Y G, Ibrahim K, Gao H J. Epitaxial growth and air-stability of monolayer antimonene on PdTe2. Adv Mater, 2017, 29: 1605407.
[7] Xiang D, Wang X, Jia C, Lee T, Guo X. Molecular-scale electronics: from concept to function. Chem Rev, 2016, 116: 4318—4440.
[8] Bailo E, Deckert V. Tip-enhanced Raman scattering. Chem Soc Rev, 2008, 37: 921—930.
[9] Kumar N, Mignuzzi S, Su W T, Roy D. Tip-enhanced Raman spectroscopy: principles and applications. EPJ Techniques and Instrumentation, 2015, 2: UNSP 9.
[10] Campion A, Kambhampati P. Surface-enhanced Raman scattering. Chem Soc Rev, 1998, 27: 241—250.
[11] Kneipp K, Wang Y, Kneipp H, Perelman L T, Itzkan I, Dasari R R, Feld M S. Single molecule detection using surface-enhanced Raman scattering (SERS). Phys Rev Lett, 1997, 78: 1667—1670.
[12] Moskovits M. Surface-enhanced spectroscopy. Reviews of Modern Physics, 1985, 57: 783—826.
[13] Deckert-Gaudig T, Taguchi A, Kawata S, Deckert V. Tip-enhanced Raman spectroscopy—from early developments to recent advances. Chem Soc Rev, 2017, 46: 4077—4110.
[14] Liu Z, Ding S Y, Chen Z B, Wang X, Tian J H, Anema J R, Zhou X S, Wu D Y, Mao B W, Xu X, Ren B, Tian Z Q. Revealing the molecular structure of single-molecule junctions in different conductance states by fishing-mode tip-enhanced Raman spectroscopy. Nat Commun, 2011, 2: 305.
[15] Zhang R, Zhang Y, Dong Z C, Jiang S, Zhang C, Chen L G, Zhang L, Liao Y, Aizpurua J, Luo Y, Yang J L, Hou J G. Chemical mapping of a single molecule by plasmon-enhanced Raman scattering. Nature, 2013, 498: 82—86.
[16] Zhang Y, Luo Y, Zhang Y, Yu Y J, Kuang Y M, Zhang L, Meng Q S, Luo Y, Yang J L, Dong Z C, Hou J G. Visualizing coherent intermolecular dipole-dipole coupling in real space. Nature, 2016, 531: 623—627.
[17] Chen H, Wan X, Wen J H, Xie W G, Kang Z W, Zeng X L, Chen H J, Xu J B. Electronic properties of MoS2-WS2 heterostructures synthesized with two-step lateral epitaxial strategy. ACS Nano, 2015, 9: 9868—9876.
[18] Melitz W, Shen J, Kummel A C, Lee S. Kelvin probe force microscopy and its application. Surface Science Reports, 2011, 66: 1—27.
[19] Palermo V, Palma M, Samorì P. Electronic characterization of organic thin films by Kelvin probe force microscopy. Advanced Materials,

2006, 18: 145—164.
[20] Fang Z, Wang Y, Schlather A E, Liu Z, Ajayan P M, de Abajo F J, Nordlander P, Zhu X, Halas N J. Active tunable absorption enhancement with graphene nanodisk arrays. Nano Lett, 2014, 14: 299—304.
[21] Saito Y, Verma P, Masui K, Inouye Y, Kawata S. Nano-scale analysis of graphene layers by tip-enhanced near-field Raman spectroscopy. Journal of Raman Spectroscopy, 2009, 40: 1434—1440.
[22] Stadler J, Schmid T, Zenobi R. Nanoscale chemical imaging of single-layer graphene. ACS Nano, 2011, 5: 8442—8448.
[23] Beams R, Cancado L G, Jorio A, Vamivakas A N, Novotny L. Tip-enhanced Raman mapping of local strain in graphene. Nanotechnology, 2015, 26: 175702.
[24] Mignuzzi S, Kumar N, Brennan B, Gilmore I S, Richards D, Pollard A J, Roy D. Probing individual point defects in graphene via near-field Raman scattering. Nanoscale, 2015, 7: 19413—19418.
[25] Everall N J. Confocal Raman microscopy: performance, pitfalls, and best practice. Appl Spectrosc, 2009, 63: 245A—262A.
[26] Budde H, Coca L N, Shi X, Ciesielski R, Lombardo A, Yoon D, Ferrari A C, Hartschuh A. Raman radiation patterns of graphene. ACS Nano, 2016, 10: 1756—1763.
[27] Everall N. Optimising image quality in 2D and 3D confocal Raman mapping. Journal of Raman Spectroscopy, 2014, 45: 133—138.
[28] Opilik L, Payamyar P, Szczerbinski J, Schutz A P, Servalli M, Hungerland T, Schluter A D, Zenobi R. Minimally invasive characterization of covalent monolayer sheets using tip-enhanced Raman spectroscopy. ACS Nano, 2015, 9: 4252—4259.
[29] Wang P, Zhang D, Li L, Li Z, Zhang L, Fang Y. Reversible defect in graphene investigated by tip-enhanced Raman spectroscopy. Plasmonics, 2012, 7: 555—561.
[30] Popov I, Durisic I, Belic M R. Designing topological defects in 2D materials using scanning probe microscopy and a self-healing mechanism: a density functional-based molecular dynamics study. Nanotechnology, 2017, 28: 495706.
[31] Sercel P C, Shabaev A, Efros A L. Photoluminescence enhancement through symmetry breaking induced by defects in nanocrystals. Nano Lett, 2017, 17: 4820—4830.
[32] Chen J, Nesterov M L, Nikitin A Y, Thongrattanasiri S, Alonso-Gonzalez P, Slipchenko T M, Speck F, Ostler M, Seyller T, Crassee I, Koppens F H, Martin-Moreno L, Garcia de Abajo F J, Kuzmenko A B, Hillenbrand R. Strong plasmon reflection at nanometer-size gaps in monolayer graphene on SiC. Nano Lett, 2013, 13: 6210—6215.
[33] Fei Z, Rodin A S, Gannett W, Dai S, Regan W, Wagner M, Liu M K, McLeod A S, Dominguez G, Thiemens M, Castro Neto A H, Keilmann F, Zettl A, Hillenbrand R, Fogler M M, Basov D N. Electronic and plasmonic phenomena at graphene grain boundaries. Nat Nanotechnol, 2013, 8: 821—825.
[34] Park K D, Raschke M B, Atkin J M, Lee Y H, Jeong M S. Probing bilayer grain boundaries in large-area graphene with tip-enhanced Raman spectroscopy. Adv Mater, 2017, 29: 1603601.
[35] Poliani E, Wagner M R, Vierck A, Herziger F, Nenstiel C, Gannott F, Schweiger M, Fritze S, Dadgar A, Zaumseil J, Krost A, Hoffmann A, Maultzsch J. Breakdown of far-field Raman selection rules by light-plasmon coupling demonstrated by tip-enhanced Raman scattering. J Phys Chem Lett, 2017, 8: 5462—5471.
[36] Jiang Q, Bao Y, Lin F, Zhu X, Zhang S, Fang Z. Spin-controlled integrated near- and far-field optical launcher. Advanced Functional Materials, 2018, 28: 1705503.
[37] Zhang W, Fang Z, Zhu X. Near-field Raman spectroscopy with aperture tips. Chem Rev, 2016, 117: 5095? 5109.
[38] Ghislandi M, Hoffmann G G, Tkalya E, Xue L, With G D. Tip-enhanced Raman spectroscopy and mapping of graphene sheets. Applied Spectroscopy Reviews, 2012, 47: 371—381.
[39] Bharadwaj P, Bouhelier A, Novotny L. Electrical excitation of surface plasmons. Phys Rev Lett, 2011, 106: 226802.
[40] Marty R, Girard C, Arbouet A, Colas des Francs G. Near-field coupling of a point-like dipolar source with a thin metallic film: Implication for STM plasmon excitations. Chemical Physics Letters, 2012, 532: 100—105.
[41] Bigourdan F, Hugonin J P, Marquier F, Sauvan C, Greffet J J. Nanoantenna for electrical generation of surface plasmon polaritons. Phys Rev Lett, 2016, 116: 106803.
[42] Andrews D L, Nunzi J-M, Ostendorf A, Boer-Duchemin E, Wang T, Le Moal E, Rogez B, Comtet G, Dujardin G. Local low-energy electrical excitation of localized and propagating surface plasmons with a scanning tunneling microscope. Conference on Nanophotonics V 2014, 9126: 91260K.
[43] Fang Z, Thongrattanasiri S, Schlather A, Liu Z, Ma L, Wang Y, Ajayan P M, Nordlander P, Halas N J, García de Abajo F J. Gated tunability and hybridization of localized plasmons in nanostructured graphene. ACS Nano, 2013, 7: 2388—2395.
[44] Gerber J A, Berweger S, O'Callahan B T, Raschke M B. Phase-resolved surface plasmon interferometry of graphene. Phys Rev Lett, 2014, 113: 055502.
[45] Nikitin A Y, Alonso-González P, Vélez S, Mastel S, Centeno A, Pesquera A, Zurutuza A, Casanova F, Hueso L E, Koppens F H L, Hillenbrand R. Real-space mapping of tailored sheet and edge plasmons in graphene nanoresonators. Nature Photonics, 2016, 10: 239—243.
[46] Yin L J, Jiang H, Qiao J B, He L. Direct imaging of topological edge states at a bilayer graphene domain wall. Nat Commun, 2016, 7: 11760.
[47] Gragnaniello L, Paschke F, Erler P, Schmitt P, Barth N, Simon S, Brune H, Rusponi S, Fonin M. Uniaxial 2D superlattice of Fe4 molecular magnets on graphene. Nano Lett, 2017, 17: 7177—7182.
[48] Huang S, Ling X, Liang L, Song Y, Fang W, Zhang J, Kong J, Meunier V, Dresselhaus M S. Molecular selectivity of graphene-enhanced Raman scattering. Nano Lett, 2015, 15: 2892—2901.
[49] Dong L, Liu P N, Lin N. Surface-activated coupling reactions confined on a surface. Acc Chem Res, 2015, 48: 2765—2774.
[50] Fang Y, Ghijsens E, Ivasenko O, Cao H, Noguchi A, Mali K S, Tahara K, Tobe Y, De Feyter S. Dynamic control over supramolecular handedness by selecting chiral induction pathways at the solution-solid interface. Nat Chem, 2016, 8: 711—717.
[51] Liu H J, Jiao L, Xie L, Yang F, Chen J L, Ho W K, Gao C L, Jia J F, Cui X D, Xie M H. Molecular-beam epitaxy of monolayer and bilayer WSe2: a scanning tunneling microscopy/spectroscopy study and deduction of exciton binding energy. 2D Materials, 2015, 2: 034004.
[52] Li B L, Wang J, Zou H L, Garaj S, Lim C T, Xie J, Li N B, Leong D T. Low-dimensional transition metal dichalcogenide nanostructures based sensors. Advanced Functional Materials, 2016, 26: 7034—7056.
[53] Li Z, Ye R, Feng R, Kang Y, Zhu X, Tour J M, Fang Z. Graphene quantum dots doping of MoS2 monolayers. Adv Mater, 2015, 27: 5235—5240.
[54] Luo Y, Chi C, Jiang M, Li R, Zu S, Li Y, Fang Z. Plasmonic chiral nanostructures: chiroptical effects and applications. Advanced

Optical Materials, 2017, 5: 1700040.
[55] Li Y, Li Z, Chi C, Shan H, Zheng L, Fang Z. Plasmonics of 2D nanomaterials: properties and applications. Adv Sci (Weinh), 2017, 4: 1600430.
[56] Choi J, Zhang H, Choi J H. Modulating optoelectronic properties of two-dimensional transition metal dichalcogenide semiconductors by photoinduced charge transfer. ACS Nano, 2016, 10: 1671—1680.
[57] Boulesbaa A, Wang K, Mahjouri-Samani M, Tian M, Puretzky A A, Ivanov I, Rouleau C M, Xiao K, Sumpter B G, Geohegan D B. Ultrafast charge transfer and hybrid exciton formation in 2D/0D heterostructures. J Am Chem Soc, 2016, 138: 14713—14719.
[58] Morgenstern M, Freitag N, Nent A, Nemes-Incze P, Liebmann M. Graphene quantum dots probed by scanning tunneling microscopy. Annalen der Physik, 2017, 529: 1700018.
[59] Gutiérrez C, Brown L, Kim C-J, Park J, Pasupathy A N. Klein tunnelling and electron trapping in nanometre-scale graphene quantum dots. Nature Physics, 2016, 12: 1069—1075.
[60] Lee J, Wong D, Velasco Jr J, Rodriguez-Nieva J F, Kahn S, Tsai H-Z, Taniguchi T, Watanabe K, Zettl A, Wang F, Levitov L S, Crommie M F. Imaging electrostatically confined Dirac fermions in graphene quantum dots. Nature Physics, 2016, 12: 1032—1036.
[61] Dhanabalan S C, Dhanabalan B, Ponraj J S, Bao Q, Zhang H. 2D-materials-based quantum dots: gateway towards next-generation optical devices. Advanced Optical Materials, 2017, 5: 1700257.
[62] Li Y, Hu Y, Zhao Y, Shi G, Deng L, Hou Y, Qu L. An electrochemical avenue to green-luminescent graphene quantum dots as potential electron-acceptors for photovoltaics. Adv Mater, 2011, 23: 776—780.
[63] Liu D, Chen X, Hu Y, Sun T, Song Z, Zheng Y, Cao Y, Cai Z, Cao M, Peng L, Huang Y, Du L, Yang W, Chen G, Wei D, Wee A T S, Wei D. Raman enhancement on ultra-clean graphene quantum dots produced by quasi-equilibrium plasma-enhanced chemical vapor deposition. Nat Commun, 2018, 9: 193.
[64] Fang Z, Zhu X. Plasmonics in nanostructures. Adv Mater, 2013, 25: 3840—3856.
[65] Li B, Zu S, Zhou J, Jiang Q, Du B, Shan H, Luo Y, Liu Z, Zhu X, Fang Z. Single-nanoparticle plasmonic electro-optic modulator based on MoS2 monolayers. ACS Nano, 2017, 11: 9720—9727.
[66] Pérez L A, Dalfovo M C, Troiani H, Soldati A L, Lacconi G I, Ibañez F J. CVD graphene transferred with Au nanoparticles: an ideal platform for TERS and SERS on a single triangular nanoplate. The Journal of Physical Chemistry C, 2016, 120: 8315—8322.
[67] Rahaman M, Rodriguez R D, Plechinger G, Moras S, Schuller C, Korn T, Zahn D R T. Highly localized strain in a MoS2/Au heterostructure revealed by tip-enhanced Raman spectroscopy. Nano Lett, 2017, 17: 6027—6033.
[68] Yan J, Ma C, Liu P, Yang G. Plasmon-induced energy transfer and photoluminescence manipulation in MoS2 with a different number of layers. ACS Photonics, 2017, 4: 1092—1100.
[69] Yu Y, Ji Z, Zu S, Du B, Kang Y, Li Z, Zhou Z, Shi K, Fang Z. Ultrafast plasmonic hot electron transfer in Au nanoantenna/MoS2 heterostructures. Advanced Functional Materials, 2016, 26: 6394—6401.
[70] Artaud A, Magaud L, Le Quang T, Guisset V, David P, Chapelier C, Coraux J. Universal classification of twisted, strained and sheared graphene moire superlattices. Sci Rep, 2016, 6: 25670.
[71] Li Z, Xiao Y, Gong Y, Wang Z, Kang Y, Zu S, Ajayan P M, Nordlander P, Fang Z. Active light control of the MoS2 monolayer exciton binding energy. ACS Nano, 2015, 9: 10158—10164.
[72] Le Quang T, Cherkez V, Nogajewski K, Potemski M, Dau M T, Jamet M, Mallet P, Veuillen J Y. Scanning tunneling spectroscopy of van der Waals graphene/semiconductor interfaces: absence of Fermi level pinning. 2D Materials, 2017, 4: 035019.
[73] Ugeda M M, Bradley A J, Shi S F, da Jornada F H, Zhang Y, Qiu D Y, Ruan W, Mo S K, Hussain Z, Shen Z X, Wang F, Louie S G, Crommie M F. Giant bandgap renormalization and excitonic effects in a monolayer transition metal dichalcogenide semiconductor. Nat Mater, 2014, 13: 1091—1095.
[74] Yu X, Rahmanudin A, Jeanbourquin X A, Tsokkou D, Guijarro N, Banerji N, Sivula K. Hybrid heterojunctions of solution-processed semiconducting 2D transition metal dichalcogenides. ACS Energy Letters, 2017, 2: 524—531.
[75] Ma Z W, Chi C, Yu Y, Zhong Z Q, Yao L H, Zhou Z K, Wang X, Han Y B, Han J B. Near-UV-enhanced broad-band large third-order optical nonlinearity in aluminum nanorod array film with sub-10 nm gaps. Opt Express, 2016, 24: 5387—5394.
[76] Park K D, Khatib O, Kravtsov V, Clark G, Xu X, Raschke M B. Hybrid tip-enhanced nanospectroscopy and nanoimaging of monolayer WSe2 with local strain control. Nano Lett, 2016, 16: 2621—2627.
[77] Cocker T L, Jelic V, Gupta M, Molesky S J, Burgess J A J, Reyes G D L, Titova L V, Tsui Y Y, Freeman M R, Hegmann F A. An ultrafast terahertz scanning tunnelling microscope. Nature Photonics, 2013, 7: 620—625.
[78] Han T, Zu S, Li Z, Jiang M, Zhu X, Fang Z. Reveal and control of chiral cathodoluminescence at subnanoscale. Nano Lett, 2018, 18: 567—572.

FANG ZheYu

FANG ZheYu is a Professor in the School of Physics, Peking University, China, received his PhD in Physics from Peking University with Prof. Xing Zhu, and worked as Postdoc at Rice University with Prof. Naomi J Halas and Prof. Peter J Nordlander. He has published more than 100 peer reviewed papers with 5000 citations. He joined Peking University in 2012 and was selected as the National Top-notch Young Professionals in 2014. His current research interests are plasmonics, near-field optics, and nanophotonic materials and devices.